Chapter 7 Decentralized Control System Design

7.1 Preliminary Considerations

7.1.1 General Concepts

From interaction analysis, we know that:

1. The difference from single-loop behavior increases as the interaction, as indicated by the magnitude of the off-diagonal gains, increases.
2. Whether the manipulated variables move a greater or lesser amount in multivariable control compared with single-loop depends on the *direction* of the set point changes. Note that this behavior is different from a single-loop case, in which only the input magnitude is important.
3. System with one-way interaction deviates less from single-loop behavior than the systems with moderate to strong transmission interaction.

Consequently, the major differences between single-loop and interactive multiloop system control are:

1. The values of the manipulated variables that satisfy the desired controlled variables must be determined simultaneously.
2. Differences between single-variable and multivariable behavior increase as the transmission interaction increases.
3. The sensitivity of the adjustments in manipulated variables to model changes can be much greater in multiloop systems than in single-loop systems.

There are two basic multivariable control approaches. The first is a straightforward extension of single-loop control to many controlled variables in a single process. This is termed multiloop control and has been applied with success for many decades. The second main category is *coordinated* or *centralized* control, in which a single control algorithm uses all measurements to calculate all manipulated variables simultaneously.

For decentralized controller design, we have to consider the effects of interaction on multivariable system behavior, assuming that the process has a controllable input-output selection. The goal for decentralized controller design is to find out how the responses of a control system are influenced by interaction. The design of multiple single-loop controllers for multivariable systems proceeds in two stages:

1. Judicious choice of loop pairing
2. Controller tuning for each individual loop

After control configuration (loop paring) been selected, the first step is to derive the transfer function for the multiloop feedback control system and determine the main differences from single-loop control.

7.1.2 Advantages and disadvantages of Decentralized Control Method

For decentralized controller design, we have to consider the effects of interaction on multivariable system behavior, assuming that the process has a controllable input-output selection. The goal for

decentralized controller design is to find out how the responses of a control system are influenced by interaction. Decentralized PID control has the following advantages:

1. It has flexibility and fault tolerance as independent loops can be turned on and off, due to operator decision or faults, without excessive degradation on the performance of the rest of loops.
2. Independent design of SISO regulators is allowed with easier online tuning.
3. The cost of implementation of a decentralized control system is significantly lower than that of a centralized controller.
4. Decentralized controllers involve far fewer parameters, resulting in a significant reduction in the time and cost of tuning.
5. They are often easier to understand by operators.
6. They tend to be less sensitive to uncertainty, for example, in the input channels.
7. Computation load in decentralized control is lesser than that in centralized control.
8. It is simplicity for implementation and manual tuning.
9. The controller structure is simple and easy to handle loop failure.
10. We can use the standard equipment.

However, if off-diagonal elements in $G(s)$ are large, then the performance with decentralized control may be poor because no attempt is made to counteract the interactions.

1. It may not work in strongly coupled systems.
2. The optimal solution is very difficult mathematically.
3. A number of pairing option is $n!$ for a $n \times n$ plant and thus increase exponentially with the size of the plant.
4. The optimal controller is in general of infinite order and may be non-unique.
5. It has a lack of flexibility for interaction adjustment and few powerful tools for its design compared with general multivariable control.

7.1.3 Summary Existing Decentralized Control Methods

Many design methods based on decentralized control have been reported in literature. The popular controller design methods are listed below.

1. The biggest log modulus (BLT) tuning approach proposed by Luyben and co-workers (Luyben, 1986, Yu, et al., 1986, Monica, et al., 1988)
2. IMC-PID Controller Based on dRI Analysis proposed by Mao-Jun He, Wen-Jian Cai and Bing-Fang Wu (He, et al., 2006)
3. Effective transfer function method in terms of NRGA interaction measurement method proposed by Qiang Xiong and Wen-Jian Cai (Q. Xiong, 2006)
4. Analytical Design by extending the generalized IMC–PID method for single input/single output (SISO) systems (Lee, et al., 2004, Vu, et al., 2007, Lee, et al., 2004, Economou, et al., 1986)

5. Simple tuning method derived from controller synthesis method (Chien, et al., 1999)
6. Ziegler–Nichols with detuning factor approach (McAvoy, 1985)
7. Sequential loop tuning approach (Shen, et al., 1994, Loh, et al., 1993, 1994, Lee, et al., 1998)
8. Nyquist stability analysis based tuning approach proposed by Dan Chen and Dale E. Seborg (Chen, et al., 2003)
9. Dominant Pole Placement method proposed by Yu Zhang, Qing-Guo Wang and K. J. Astrom (Zhang, et al., 2005, Wang, et al., 1998)
10. Independent Design method (Skogestad, et al., 1989)
11. Multiloop PID Controller Tuning approach based on Gain and Phase Margin Specifications (Ho, et al., 1997)
12. Singular Value Decomposition (SVD) based method proposed by Goshaidas Ray, A.N. Prasad and T.K. Bhattacharyya (Raya, et al., 1999)

In this Chapter, we will introduce the first three controller design methods in the above list. The selection of BLT tuning method is because it is the first approach to the decentralized or multi-loop multivariable control. It is also a benchmark method for decentralized control. The equivalent transfer function methods are interesting because they considers four combination modes of gain and phase changes for a particular loop when other loops are closed. Consequently, the decentralized controllers can be independently designed by employing the single loop tuning techniques. The method is simple, straightforward, easy to understood and implemented by field engineers.

7.2 Biggest Log Modulus Tuning Method

A common way is to first design individual controller for each control loop by ignoring all interactions, and then detune each loop by a detuning factor. Luyben proposed the Biggest Log-modulus Tuning (BLT) method for multiloop PI/PID controllers. In the BLT method, the well-known Ziegler-Nichols rule is modified with the inclusion of the detuning factors, which determines the tradeoff between stability and performance of the system.

7.2.1 BLT method for SISO systems

The closed-loop characteristic equation for a SISO system is

$$1 + g(s)g_c(s) = 0$$

Where, g is the open-loop process transfer function and g_c is the feedback controller transfer function. A Nyquist (or Bode or Nichols) plot of $g(i\omega)g_c(i\omega)$ is made as the frequency ω goes from zero to infinity. The number of encirclements of the (-1, 0) point is equal to the number of roots of the closed-loop characteristic equations that lie in the right half of the s plane if the open-loop system is stable. Thus, if the (-1, 0) point is encircled, the closed-loop system is unstable.

The farther away from the $(-1, 0)$ point, the system is more stable. One commonly used measure of the distance of the $g(i\omega)g_c(i\omega)$ contour from the $(-1, 0)$ point is the maximum closed-loop log modulus (L_c^{max}). The closed-loop log modulus is the magnitude of the closed-loop servo-transfer function.

$$L_c = 20\log\left|\frac{gg_c}{1+gg_c}\right| \tag{7.2.1}$$

A commonly used specification is +2 dB for L_c^{max}. A value of the controller gain (K_c) is selected, and L, is plotted as a function of frequency. The maximum value of L_c is determined, and if it is less than +2 dB, the gain is increased. This procedure is repeated until the biggest log modulus for all frequencies is +2 dB. A Nichols chart can be used alternatively to transform $g(j\omega)g_c(j\omega)$ information into L_c results.

7.2.2 BLT method for MIMO systems

Consider an open loop stable multivariable system with n inputs and n outputs as shown in the transfer functions and the controllers are typically in the form of

$$g_{ij} = \frac{K_{ij}(\tau_{1ij}s+1)e^{-D_{ij}s}}{(\tau_{2ij}s+1)(\tau_{3ij}s+1)(\tau_{4ij}s+1)} \tag{7.2.2}$$

The feedback controller matrix $G_c(s)$ is diagonal since we are using n SISO controllers

$$G_c(s) = \begin{bmatrix} g_{c1}(s) & 0 & 0 & ..... & 0 \\ 0 & g_{c2}(s) & 0 & ... & 0 \\ 0 & 0 & g_{c3}(s) & ... & 0 \\ . & . & . & & . \\ . & . & . & & . \\ 0 & 0 & 0 & ... & g_{cn}(s) \end{bmatrix} \tag{7.2.3}$$

where

$$g_{ci}(s) = K_P + \frac{K_I}{s} + K_D s \tag{7.2.4}$$

respectively.

The first step in BLT tuning method is to calculate the Ziegler-Nichols setting for each individual loop. The ultimate gain K_u and ultimate frequency ω_u of each diagonal transfer function are calculated in the classical SISO way. To do this numerically, a value of the frequency is guessed. The phase angle is calculated, and frequency is varied until the phase angle is equal to -180°. This frequency is ω_u. The ultimate gain is the reciprocal of the real part of $g_{ii}(s)$ at ω_u. There are several ways to find the ultimate data settings, including the method of sustained oscillations, the relay experiment, or even straightforward Nyquist plotting using software like MATLAB.

Next, a factor F is assumed. Typical values vary from 2 to 5**.** The gains of all feedback controllers K_C are calculated by dividing the Ziegler-Nichols gain K_{ZN_i} by the factor F,

$$K_{Ci} = \frac{K_{ZN_i}}{F} \tag{7.2.5}$$

where,

$$K_{ZN_i} = \frac{K_{u_i}}{2.2} \tag{7.2.6}$$

The reset times *(* τ_I *)* of all controllers are calculated by multiplying the Ziegler-Nichols reset times (τ_{ZN}) by the same factor F,

$$\tau_{Ii} = F\tau_{ZN_i} \tag{7.2.7}$$

where,

$$\tau_{ZN_i} = \frac{2\pi}{1.2\omega_{ui}} \tag{7.2.8}$$

The F factor can be considered a detuning factor, which is applied to all loops. The larger the value of *F,* the more stable but the more sluggish the system will be to the set point and load responses.

To yield a value of *F,* we outline a method below which gives a reasonable compromise between stability and performance in multivariable systems.

The closed-loop system can be expressed by

$$y = \left[I + GG_c\right]^{-1} GG_c r \tag{7.2.9}$$

Since the inverse of a matrix has the determinant of the matrix in the denominator, the closed-loop characteristic equation of the multivariable system is the scalar equation

$$\det(I + GG_c) = 0 \tag{7.2.10}$$

The number of right half plane zeros of the closed-loop characteristic equation can be found by plotting the left side of Equation (7.2.10) as a function of frequency and looking at the encirclements of the origin. In order to make this multivariable plot look just like the SISO scalar Nyquist plot, we subtract one from Equation (7.2.10) and look at the encirclements of the $(-1,0)$ point. It is convenient to define a new function

$$W(s) = -1 + \det(I + GG_c)(s) \tag{7.2.11}$$

W is plotted as a function of frequency. The closer W approaches the $(-1,0)$ point, the closer the multivariable system is to closed-loop instability. The quantity

$$\frac{W(s)}{1 + W(s)} \tag{7.2.12}$$

will be similar to the closed-loop servo-transfer function for a SISO loop

$$\frac{g(s)g_c(s)}{1+g(s)g_c(s)} \tag{7.2.13}$$

Therefore, based on intuition and empirical grounds, a multivariable closed-loop log modulus L_{cm} are defined as

$$L_{cm} = 20 \times \log\left|\frac{W}{1+W}\right| \tag{7.2.14}$$

The proposed tuning method is based on varying the factor F until the biggest log modulus $(L_{cm})^{\max}$ is equal to some reasonable number. Thus, the proposed tuning method is called the biggest log modulus tuning (BLT).

Now we must determine what is a reasonable value to use for $(L_{cm})^{\max}$ for different orders of the systems. For a SISO system where $N = 1$, we know from long experience that a value of $+2$ dB for $(L_{cm})^{\max}$ gives reasonable time domain responses for set point and load disturbances. The best tuning criterion for this method is

$$(L_{cm})^{\max} = 2N \tag{7.2.15}$$

For $N = 1$, this reduces to the classical +2dB criterion. For a 4×4 system, a $(L_{cm})^{\max}$ of 8 should be used. These empirical findings suggest that the higher the order of the system, the more under damped the closed-loop system must be to achieve reasonable responses.

This tuning method should be viewed as giving preliminary controller settings, which can be used as a benchmark for comparative studies. Note that this procedure guarantees that the system is stable with all controllers on automatic and that each individual loop will be stable if all others are on manual. Thus, a portion of the integrity question is automatically answered.

The method weighs each loop equally; i.e., each loop is detuned by the same factor *F*. If it is more important to keep tighter control of some variable than the others, the method can be easily modified by using different weighting factors for different controlled variables. The less-important loop could be detuned more than the more-important loop.

We will summarize BLT-1 tuning procedures mentioned above as follow.

1. Compute the Ziegler-Nichols tuning parameters of the diagonal elements of the process transfer function matrix $g_{ii}(s)$ as though the diagonal elements represented SISO systems.
2. Choose a detuning factor F . F should be greater than one.
3. Compute K_{Ci} , and τ_{Ii} for each loop by

$$K_{Ci} = \frac{K_{ZN_i}}{F} \tag{7.2.16}$$

$$\tau_{Ii} = F\tau_{ZN_i} \tag{7.2.17}$$

where K_{ZN_i} and τ_{ZN_i} are the Ziegler-Nichols PI values.

4. Calculate the function W over the appropriate frequency range (i.e., near the $(-1,0)$ point), where

$$W = -1 + \det\left[I + G(j\omega)G_c(j\omega)\right] \tag{7.2.18}$$

5. Compute the function $L_c(j\omega)$ where

$$L_c(j\omega) = 20 \times \log\left|\frac{W}{1+W}\right| \tag{7.2.19}$$

6. Adjust F until the peak in the L_c log modulus curve L_{cm} is equal to $2N$,i.e., $L_c^{\max} = 2N$, where L_{cm} is the biggest log modulus in the L_c curve and N is the number of SISO loops in the multivariable system.

It is important when applying this procedure to confirm the form of the Nyquist plot of the function W , because the log modulus function merely denotes nearness to the critical point. An unstable system could be tuned to a maximum log modulus of $2N$ because it encircles the $(-1,0)$ point but is not near it.

After tuning by BLT, derivative action can be incorporated through the steps that follow. We will consider derivative action for SOPTD processes in this dissertation.

1. Choose a second detuning factor F_D. It should be greater than one.

2. Compute τ_{Di}, where

$$\tau_{Di} = \frac{\tau_{Di-ZN}}{F_D} \tag{7.2.20}$$

and τ_{Di-ZN} is the Ziegler-Nichols value for τ_{Di} and is equal to

$$\tau_{Di-ZN} = 0.125 \times P_u . \tag{7.2.21}$$

3. Repeat steps 4 and 5 of the BLT-1 procedure. Change F_D until $L_c^{\max}$ is minimized, maintaining $F_D \geq 1$. The trivial case may result where $L_c^{\max}$ is minimized for $F_D = \infty$, i.e., no derivative action.

4. Reduce F_D, and repeat steps 3, 4, and 5 of the BLT-1 procedure until $L_c^{\max} = 2N$.

5. Repeat steps 4 and 5 above until no further reduction in F is possible. By this process, we are shifting the phase angle of the closed-loop characteristic equation Nyquist contour by tuning the derivative terms so that they have the greatest effect near the closed-loop resonant frequency.

Note that this procedure guarantees that the system is stable with all controllers on automatic and that each individual loop will be stable if all others are on manual. Thus, a portion of the integrity question is automatically answered.

The method weighs each loop equally; i.e., each loop is detuned by the same factor *F*. If it is more important to keep tighter control of some variable than others, the method can be easily modified

by using different weighting factors for different controlled variables. The less-important loop could be detuned more than the more-important loop.

The simplicity of this method is its major advantage. Nevertheless, the disadvantage results from the fact that loop performance and stability can not be clearly defined through the detuning procedures. Generally, this class method only provides reasonable preliminary controller settings with guaranteed closed-loop stability.

7.2.3 Examples

Example 7.2.1 Wood and Berry binary distillation column plant

$$\begin{bmatrix} X_D(s) \\ X_B(s) \end{bmatrix} = \begin{bmatrix} \dfrac{12.8e^{-s}}{1+16.7s} & \dfrac{-18.9e^{-3s}}{1+21s} \\ \dfrac{6.6e^{-7s}}{1+10.9s} & \dfrac{-19.4e^{-3s}}{1+14.4s} \end{bmatrix} \begin{bmatrix} R(s) \\ S(s) \end{bmatrix} + \begin{bmatrix} \dfrac{3.8e^{-8.1s}}{1+14.9s} \\ \dfrac{4.9e^{-3.4s}}{1+13.2s} \end{bmatrix} F(s).$$

where $X_D(s)$ and $X_B(s)$ are the overhead and bottom compositions of methanol, respectively; R is the reflux flow rate and S is the steam flow to the reboiler; F is the feed flow rate, a load disturbance. It is a typical TITO plant with strong interactions and significant time delays.

Using BLT method, each loop is also detuned by same factor 4. The resultant PI controllers are listed in the Table. The close loop responses for the controller is as shown in the Figure, where the unit set-points change in r_1 at t=0 and r_2 at t=800.

Controller for Wood and Berry

Controller	$K_{c,ii}$	$\tau_{i,ii}$
Loop 1	0.375	8.29
Loop 2	-0.075	23.6

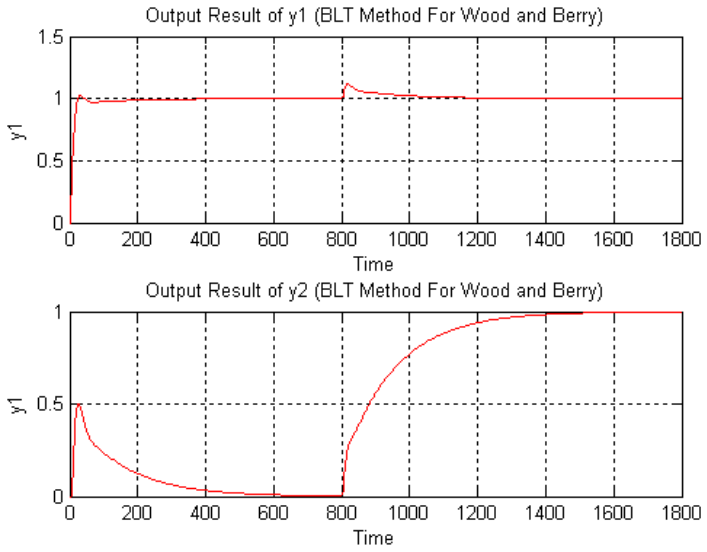

Fig. 7.2.3 Close loop response for Wood and Berry by using BLT method

7.3 Equivalent Transfer Function methods

7.3.1 Equivalent Transfer Functions

From Chapter 4, we know there are two forms of EFTs:

1. EFT based on RNGA

$$\hat{g}_{ij}(s) = \frac{k_{ij}}{\lambda_{ij}} \times \frac{1}{\gamma_{ij} T_{ij} s + 1} e^{-\gamma_{ij} L_{ij} s} \quad \text{for } i, j = 1, 2, \cdots n \tag{7.3.1}$$

for FOPTD, and

$$\hat{g}_{ij}(s) = \frac{k_{ij}}{\lambda_{ij}} \times \frac{\omega_{n,ij}^2}{s^2 + 2\gamma_{ij}\zeta_{ij}\omega_{n,ij} s + \omega_{n,ij}^2} e^{-\gamma_{ij}\theta_{ij} s} \quad \text{for } i, j = 1, 2, \cdots n \tag{7.3.2}$$

For SOPTD, respectively.

2. ETF based on DRGA approximation

$$\hat{g}_{ij}(s) = \hat{k}_{ij} g_{ij}^0(s) e^{-\hat{\theta}_{ij} s} = k_{ij} \times k_{\lambda_{ij}} g_{ij}^0(s) e^{-(\theta_{ij} + \theta_{\lambda_{ij}}) s} \tag{7.3.3}$$

The ETFs based design is to design controllers purely based on the information provided by the ETFs without inferring to the other loops. In this way, the design procedure can be much simplified.

7.3.2 Determine Equivalent Transfer Functions for Integrity

In decentralized control, the task for controller design becomes to determine $g_{c,ii}(s)\hat{g}_{ii}(s)$ such that the closed-loop has good dynamic performance.

For control system integrity, the steady state gain and the phase in ETFs must take different values for different combination of $k_{\lambda_{ii}}$ and $\theta_{\lambda_{ii}}$ (λ_{ii} and γ_{ii} for RNGA). As the effects of λ_{ii} is equivalent to the inverse of $k_{\lambda_{ii}}$ and $\gamma_{ii} - 1$ is equivalent to $\theta_{\lambda_{ii}}$, we will use controller design for RNGA based ETF to explain the integrity issues.

Recall that

$$\hat{k}_{ii} = \frac{k_{ii}}{\lambda_{ii}}, \qquad \hat{\sigma}_{ii} = \gamma_{ii}\sigma_{ii} \tag{7.3.4}$$

and $\hat{g}_{ii}(s)$ given as in (7.3.1) to (7.3.2), the ETF for each individual case is determined based on the integrity requirement (the controller is no more aggressive than single loop without interaction):

Case 1: $\lambda_{ii} < 1,\ \gamma_{ii} \le 1$, Figures 7.3.1. We have $\hat{k}_{ii} > k_{ii}$, and $\hat{\sigma}_{ii} \le \sigma_{ii}$.

- $\hat{k}_{ii} > k_{ii}$, the steady state gain when the other loops closed is bigger that of when the other loops open. Since the retaliatory effect from the other loops magnifies the main effect of u_i

on y_i, we need to increase the original steady state gain in order to reduce the controller gain in controller design to assure system stability, i.e.,

$$\hat{k}_{ii} = k_{ii}/\lambda_{ii} \ . \tag{7.3.5}$$

- $\hat{\sigma}_{ii} \le \sigma_{ii}$, the average residence time when the other loops closed is smaller than that of when other loops open. The smaller average residence time will make the critical frequency in frequency domain shift to the right and increase the phase margin. However, by considering control system integrity (not to design a controller according to the new crossover frequency such that the system has better performance), the time delay need to be kept as before, i.e., $\hat{\sigma}_{ii} = \sigma_{ii}$.

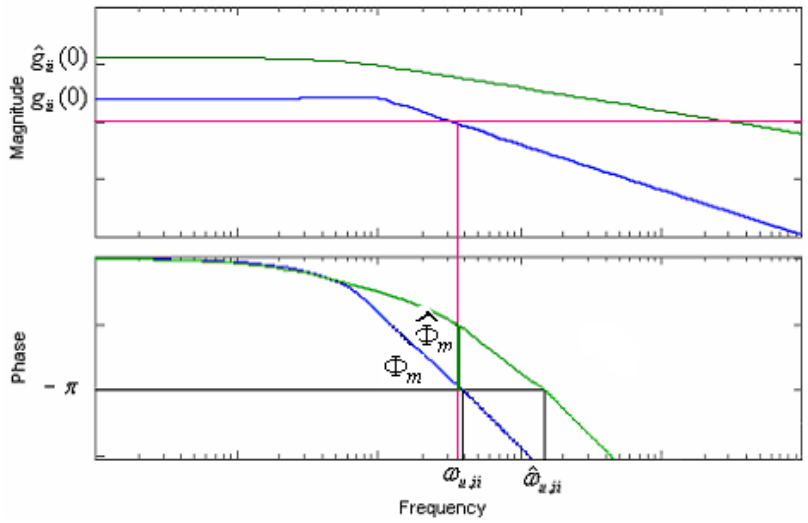

Figure 7.3.1 $\lambda_{ii} < 1,\ \gamma_{ii} \le 1$

Case 2: $\lambda_{ii} < 1,\ \gamma_{ii} > 1$, Figures 7.3.2. We have $\hat{k}_{ii} > k_{ii}$, and $\hat{\sigma}_{ii} > \sigma_{ii}$.

- $\hat{k}_{ii} > k_{ii}$, same as in Case 1, Equation (7.3.5)
- $\hat{\sigma}_{ii} > \sigma_{ii}$, the average residence time when the other loops closed is bigger than that of the other loops open. The enlarged average residence time will make the critical frequency in frequency domain shift to the left and reduce the phase margin. In this case, the average residence time is determined by:

$$\hat{\sigma}_{ii} = \gamma_{ii}\sigma_{ii} \ .$$

Implies that

$$\hat{T}_{ii} = \gamma_{ii} T_{ii} \ and \ \hat{L}_{ii} = \gamma_{ii} L_{ii} \tag{7.3.6}$$

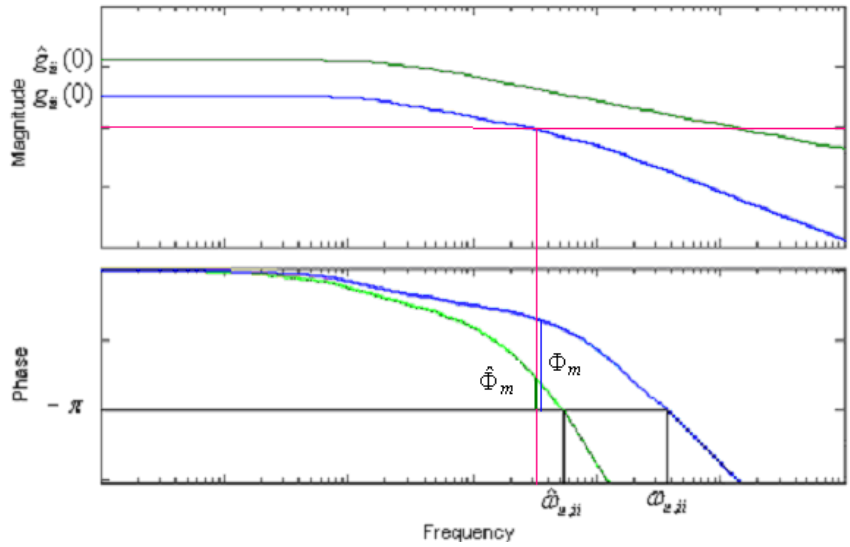

Figure 7.3.2 $\lambda_{ii} < 1,\ \gamma_{ii} > 1$

Case 3: $\lambda_{ii} \geq 1,\ \gamma_{ii} \leq 1$, Figures 7.3.3. We have $\hat{k}_{ii} \leq k_{ii}$, and $\hat{\sigma}_{ii} \leq \sigma_{ii}$.

- $\hat{k}_{ii} \leq k_{ii}$, the steady state gain when the other loops closed is smaller than that of when the other loops open. Even the retaliatory effect from other loops acts in opposition to the main effect of u_i on y_i, the controller gain cannot enlarged for better performance due to system integrity consideration. Hence, the gain should be unchanged, i.e., $\hat{k}_{ii} = k_{ii}$.
- $\hat{\sigma}_{ii} \leq \sigma_{ii}$, same as in Case 1, i.e., $\hat{\sigma}_{ii} = \sigma_{ii}$.

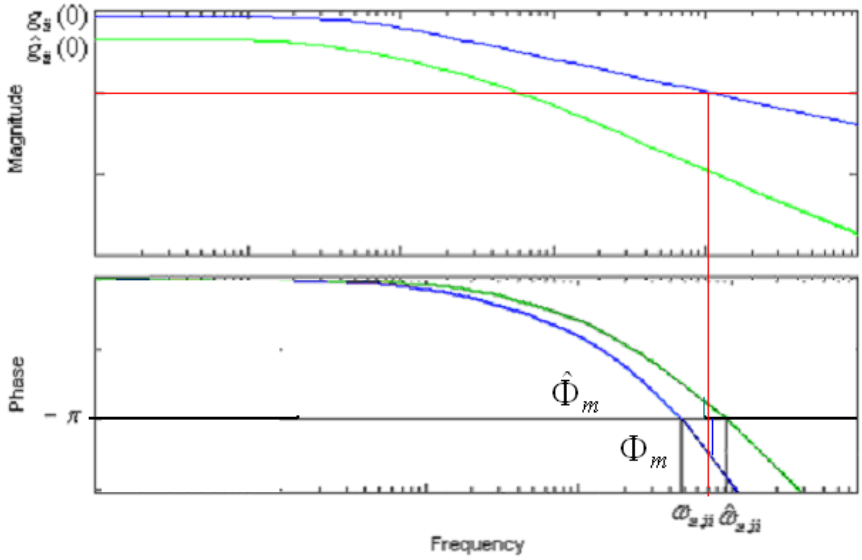

Figure 7.3.3 $\lambda_{ii} \geq 1,\ \gamma_{ii} \leq 1$

Case 4: $\lambda_{ii} \geq 1,\ \gamma_{ii} > 1$, Figure 7.3.4. We have $\hat{k}_{ii} \leq k_{ii}$, and $\hat{\sigma}_{ii} > \sigma_{ii}$.

- $\hat{k}_{ii} \leq k_{ii}$, same as in Case 3, i.e., $\hat{k}_{ii} = k_{ii}$.

- $\hat{\sigma}_{ii} > \sigma_{ii}$, same as in Case 2, i.e., $\hat{\sigma}_{ii} = \gamma_{ii}\sigma_{ii}$.

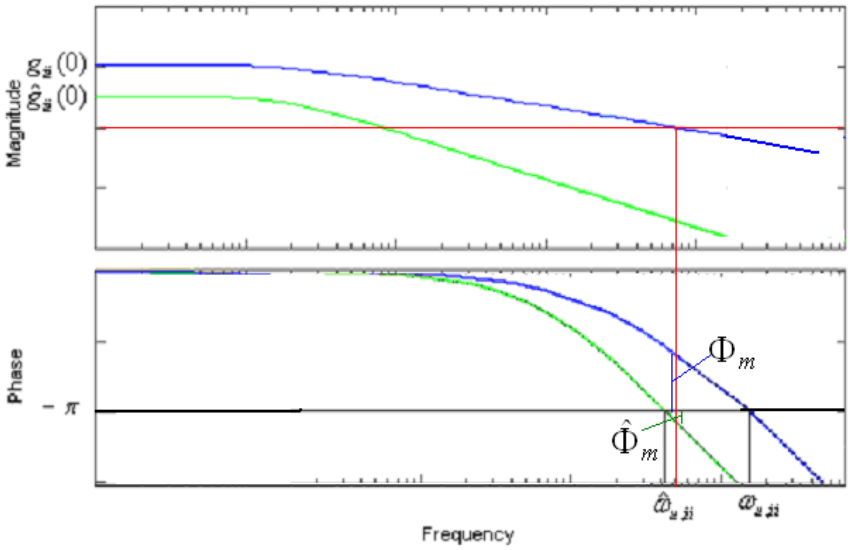

Figure 7.3.4 $\lambda_{ii} \geq 1,\ \gamma_{ii} > 1$

7.3.3 Controller Design

Integrity property can be preserved by decentralize control scheme using any existing single loop control techniques, if the ETFs are obtained by changing parameters as:

$$\begin{array}{ll} \lambda_{ii} < 1 & \hat{k}_{ii} = k_{ii} / \lambda_{ii} \\ \gamma_{ii} > 1 & \hat{\sigma}_{ii} = \gamma_{ii}\sigma_{ii} \\ \text{Otherwise} & \text{no change} \end{array}$$

For FOPTD loop transfer functions and for different combination of λ_{ii} and γ_{ii} modes, the ETF $\hat{g}_{ii}(s)$ has the form

$$\hat{g}_{ii}(s) = \begin{cases} \dfrac{k_{ij}}{\lambda_{ij}} \times \dfrac{1}{T_{ij}s+1} e^{-L_{ij}s}, & \lambda_{ii} < 1,\ \gamma_{ii} \leq 1 \\ \dfrac{k_{ij}}{\lambda_{ij}} \times \dfrac{1}{\gamma_{ij}T_{ij}s+1} e^{-\gamma_{ij}L_{ij}s}, & \lambda_{ii} < 1,\ \gamma_{ii} > 1 \\ \dfrac{k_{ij}}{T_{ij}s+1} e^{-L_{ij}s}, & \lambda_{ii} \geq 1,\ \gamma_{ii} \leq 1 \\ \dfrac{k_{ij}}{\gamma_{ij}T_{ij}s+1} e^{-\gamma_{ij}L_{ij}s}, & \lambda_{ii} \geq 1,\ \gamma_{ii} > 1 \end{cases} \tag{7.3.7}$$

Now, let the PID controller of the form

$$g_{c,ii}(s) = K_{p,ii} + \frac{K_{I,ii}}{s} + K_{D,ii}s \tag{7.3.8}$$

As a example, we can use the gain and phase margin method given in reading materials to design controllers based on the ETFs. The ETFs together with PID controller parameters based on gain and phase margin method for FOPTD loop transfer functions are given in Tables 7.3.1.

Table 7.3.1. ETFs and PID controllers for gain and phase margin method

Mode	$\hat{g}_{ii}(s)$	$k_{P,ii}$	$k_{I,ii}$
$\lambda_{ii}<1$, $\gamma_{ii}\le 1$	$\frac{k_{ij}}{\lambda_{ij}}\times\frac{1}{T_{ij}s+1}e^{-L_{ij}s}$	$\frac{\pi\lambda_{ii}T_{ii}}{2A_{m,i}L_{ii}k_{ii}}$	$\frac{\pi\lambda_{ii}}{2A_{m,i}L_{ii}k_{ii}}$
$\lambda_{ii}<1$, $\gamma_{ii}>1$	$\frac{k_{ij}}{\lambda_{ij}}\times\frac{1}{\gamma_{ij}T_{ij}s+1}e^{-\gamma_{ij}L_{ij}s}$	$\frac{\pi\lambda_{ii}T_{ii}}{2A_{m,i}L_{ii}k_{ii}}$	$\frac{\pi\lambda_{ii}}{2A_{m,i}\gamma_{ii}L_{ii}k_{ii}}$
$\lambda_{ii}\ge 1$, $\gamma_{ii}>1$	$\frac{k_{ij}}{\gamma_{ij}T_{ij}s+1}e^{-\gamma_{ij}L_{ij}s}$	$\frac{\pi T_{ii}}{2A_{m,i}\theta_{ii}k_{ii}}$	$\frac{\pi}{2A_{m,i}\gamma_{ii}L_{ii}k_{ii}}$
$\lambda_{ii}\ge 1$, $\gamma_{ii}\le 1$	$\frac{k_{ij}}{T_{ij}s+1}e^{-L_{ij}s}$	$\frac{\pi T_{ii}}{2A_{m,i}L_{ii}k_{ii}}$	$\frac{\pi}{2A_{m,i}L_{ii}k_{ii}}$

Remark: If the response is lag-dominant, i.e. if $T_{ii}>8L_{ii}$ approximately, then the lag-dominant processes may instead be approximated by a pure first order transfer function by the following two first-order Taylor approximations of a time delay transfer function:

$$e^{-L_{ii}s}\approx 1-L_{ii}s \text{ and } e^{-L_{ii}s}=\frac{1}{e^{L_{ii}s}}\approx\frac{1}{1+L_{ii}s}$$

Then, according to the half-rule, the equivalent transfer function

$$\begin{aligned}\hat{g}_{ii}(s)&=\frac{k_{ii}}{\lambda_{ii}}\times\frac{1}{\gamma_{ii}T_{ii}s+1}e^{-\gamma_{ii}L_{ii}s}\\&\approx\frac{k_{ii}\big/\lambda_{ii}}{\gamma_{ii}\left(T_{ii}+\frac{L_{ii}}{2}\right)s+1}\end{aligned}\tag{7.3.9}$$

The simple direct synthesis method can then be used by specify the desired closed loop behavior as

$$q_{ii}(s)=\frac{1}{\tau_{r,ii}s+1}\tag{7.3.10}$$

and,

$$g_{c,ii}=\frac{1}{\tau_{r,ii}sg_{ii}}=\frac{\lambda_{ii}\gamma_{ii}\left(T_{ii}+\frac{L_{ii}}{2}\right)}{\tau_{r,ii}k_{ij}}+\frac{1}{\tau_{r,ii}k_{ii}s}\tag{7.3.11}$$

A PI controller; where $\tau_{r,ii}$ is the tuning parameter. Even though $\tau_{r,ii}$ can be made arbitrary small, too small $\tau_{r,ii}$ should be avoided as smaller $\tau_{r,ii}$ requires bigger control efforts which may cause

actuator saturation and instability. The rule of thumb is that $\tau_{r,ii}$ be selected close to the loop dominant time constant.

7.3.4 Examples

Example 7.3.1. Continue with Example 7.2.1.

$$\Lambda = \begin{bmatrix} 0.7087 & 0.2913 \\ 0.2913 & 0.7087 \end{bmatrix}, \text{ and } \Gamma = \begin{bmatrix} 1.0151 & 0.9633 \\ 0.9633 & 1.0151 \end{bmatrix}.$$

Since $\lambda_{ii} < 1$ and $\gamma_{ii} > 1$ for $i = 1, 2$, ETFs for two loop are

$$\hat{g}_{11}(s) = \frac{32.3003}{4.572s + 1} e^{-0.2014s} \quad \text{and} \quad \hat{g}_{22}(s) = \frac{8.1844}{1.801s + 1} e^{-0.4015s},$$

respectively.

The REA based Decentralized Controller (REA-DCC) together with other methods are listed in Table 7.3.3.

Table 7.3.3. Decentralized Controllers for Example 7.3.1

Controller	REA-DCC		Luyben		Chien et al.		Loh et al.	
	$k_{p,ii}$	$\tau_{i,ii}$	$k_{p,ii}$	$\tau_{i,ii}$	$k_{p,ii}$	$\tau_{i,ii}$	$k_{p,ii}$	$\tau_{i,ii}$
Loop 1	0.2208	4.5720	0.210	2.26	0.263	1.42	0.620	0.60
Loop 2	0.1722	1.8010	0.175	4.25	0.163	1.77	0.247	1.78

Figure 7.3.5 shows the responses for different control methods with unit set-points change in r_1 at t=0 and r_2 at t=20 and the proposed design method gives the best performance.

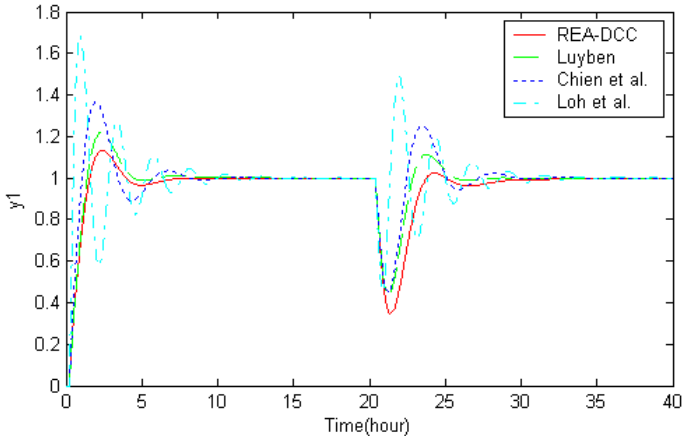

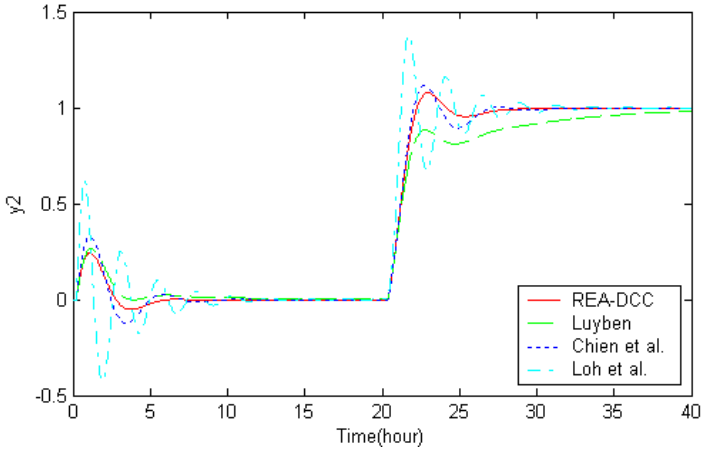

Figure7.3.5 Closed-loop responses of decentralized control for Example 7.3.1

7.4 Comparison Study

7.4.1 Distillation Column 2×2 Model

Vinante and Luyben System with transfer function matrix is given as

$$G(s)=\begin{bmatrix} \dfrac{-2.2e^{-s}}{7s+1} & \dfrac{1.3e^{-0.3s}}{7s+1} \\ \dfrac{-2.8e^{-1.8s}}{9.5s+1} & \dfrac{4.3e^{-0.35s}}{9.2s+1} \end{bmatrix}.$$

$$k=\begin{bmatrix} -2.2 & 1.3 \\ -2.8 & 4.3 \end{bmatrix} \text{ and } \Lambda=\begin{bmatrix} 1.6254 & -0.6254 \\ -0.6254 & 1.6254 \end{bmatrix}$$

respectively. Using NI screening tool and the RGA values for possible pairing is 1-1, 2-2.

BLT: The ultimate values and Ziegler-Nichols tuning parameters of the diagonal elements of this process transfer function matrix are shown in Table 7.4.1.

Table 7.4.1 The ultimate values and ZN tuning parameters

Parameters	Loop 1	Loop 2
K_u	-5.2912	9.7507
ω_u	1.6568	4.5561
K_{ZN}	-2.4051	4.4322
τ_{ZN}	3.1603	1.1492

We assume that F is equal to 2.3, controller parameters can be calculated by using tuning factor F . See Table 7.4.1 for controller values. We do not try to find τ_D in this case. However, we

will find it in the later two cases by using F_d derivative factor.

ETF based on DRGA: The first step is to calculate critical frequencies of the diagonal transfer functions, then calculate

$$\rho_{11,1}(j0.5) = 0.3900 - j0.3206$$
$$\rho_{22,1}(j1.4286) = 0.0033 + j0.0476$$

respectively. Subsequently MMF can be calculated as

$$\rho_{11,1} = 1.4265e^{-0.6800s}$$
$$\rho_{22,1} = 1.0044e^{-(-0.0498)s}$$

Then the equivalent transfer functions of both control loops are constructed as

$$\hat{g}_{11} = \frac{-3.138e^{-1.68s}}{7s+1} \quad \text{and} \quad \hat{g}_{22} = \frac{4.319e^{-0.35s}}{9.2s+1}.$$

Consequently, the decentralized PI controllers parameters are determined by IMC are shown in Table **7.4.**2 and Figure 7.4.1 shows the responses for each control loop.

NRGA: In this method, the gain and phase margin for all loops are specified to be 3 and $\pi/3$, respectively. These margins are generally regarded as making the best compromise between performance and robustness in process control.

The RGA, RNGA and RARTA are

$$\Lambda = \begin{bmatrix} 1.6254 & -0.6254 \\ -0.6254 & 1.6254 \end{bmatrix}, \quad \Phi = \begin{bmatrix} 1.5939 & -0.5939 \\ -0.5939 & 1.5939 \end{bmatrix}$$

and

$$\Gamma = \begin{bmatrix} 0.9806 & 0.9497 \\ 0.9497 & 0.9806 \end{bmatrix}$$

respectively.

Since $\lambda_{ii} > 1$ and $\gamma_{ii} < 1$ for $i = 1, 2$, we do not need to detune and ETFs for two loops are

$$\hat{g}_{11}(s) = \frac{-2.2e^{-s}}{7s+1} \text{ and } \quad \hat{g}_{22}(s) = \frac{4.3e^{-0.35s}}{9.2s+1}$$

respectively.

The controller parameters for all methods are shown in Table 7.4.2.

Table 7.4.2 Decentralized Controllers for VL System

Method	Loop	K_C	τ_I	τ_D
BLT	1	-1.0502	7.2372	0

	2	1.9354	2.6318	0
SIMC	1	-0.7048	7.0000	0
	2	1.9449	4.2000	0
ERGA	1	-1.6660	7.0000	0
	2	3.2007	9.2000	0

Figure 7.4.1 show the responses for all control methods with unit set points change in r_1 at t=0 and r_2 at t=50.

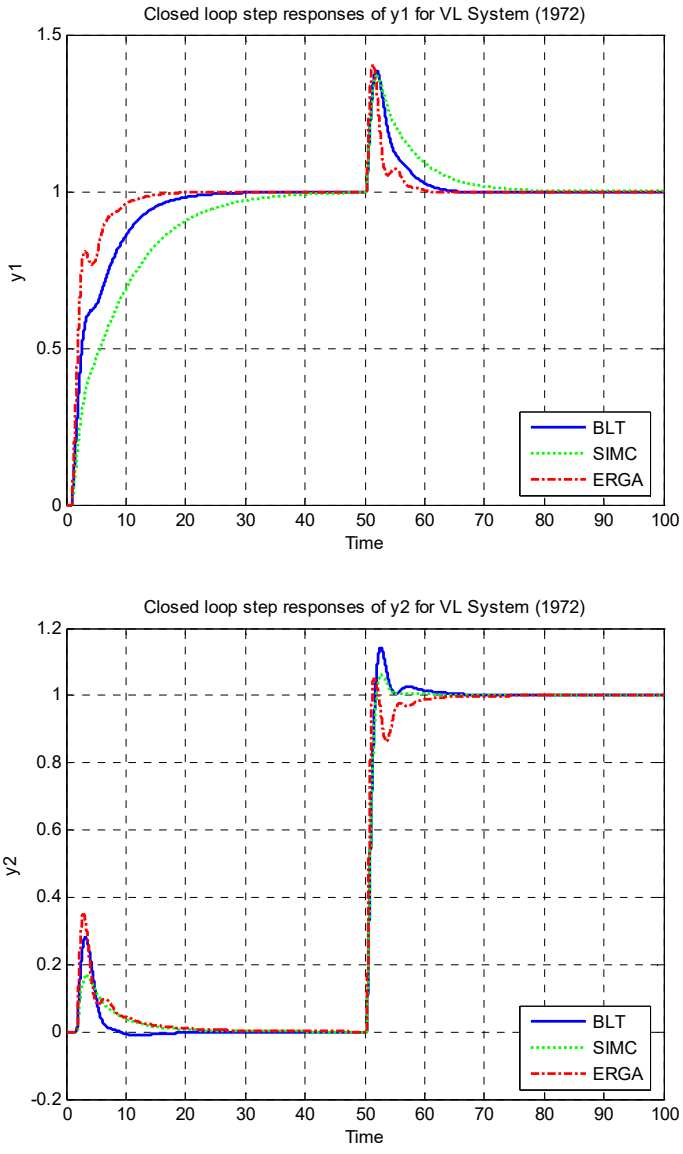

Figure 7.4.1 Closed loop step responses of VL System

7.4.2 Distillation Column 3×3 Model (Ogunnaike and Ray System)

The transfer function matrix is given as

$$G(s)=\begin{bmatrix} \dfrac{0.66e^{-2.6s}}{6.7s+1} & \dfrac{-0.61e^{-3.5s}}{8.64s+1} & \dfrac{-0.0049e^{-s}}{9.06s+1} \\ \dfrac{1.11e^{-6.5s}}{3.25s+1} & \dfrac{-2.36e^{-3s}}{5s+1} & \dfrac{-0.01e^{-1.2s}}{7.09s+1} \\ \dfrac{-34.68e^{-9.2s}}{8.15s+1} & \dfrac{46.2e^{-9.4s}}{10.9s+1} & \dfrac{0.87(11.61s+1)e^{-s}}{(3.89s+1)(18.8s+1)} \end{bmatrix}.$$

Since SIMC and ETF only use the standard transfer function models such as FOPTD and SOPTD, we need to do parameter estimation for $g_{33}(s)$ in the system mentioned above. We can use the theoretical or empirical methods to estimate parameters. The new transfer function model in the form of FOPTD is

$$g_{33new}=\frac{0.87e^{-s}}{10s+1}$$

and the following diagram shows the comparison of step responses for both transfer functions.

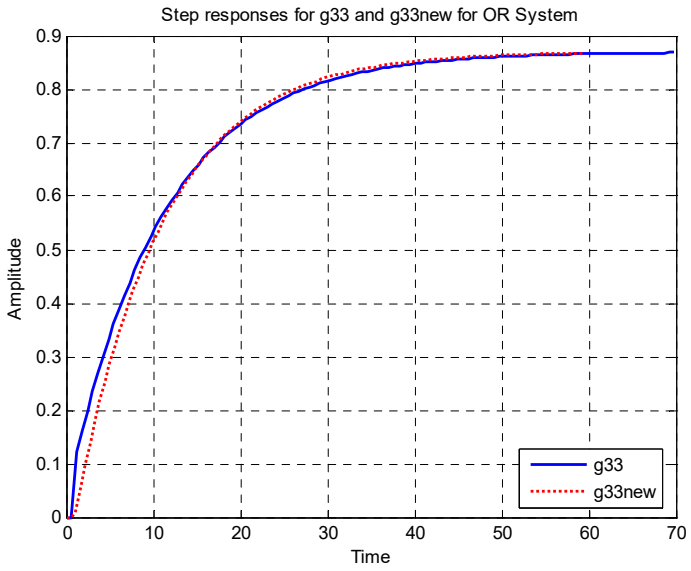

Figure 7.4.2 Step responses for g33 and g33new for OR System

BLT: The DC gain and RGA values for the best pairing are

$$k=\begin{bmatrix} 0.6600 & -0.6100 & -0.0049 \\ 1.1100 & -2.3600 & -0.0100 \\ -34.6800 & 46.2000 & 0.8700 \end{bmatrix} \text{ and } \Lambda=\begin{bmatrix} 2.0084 & -0.7220 & -0.2864 \\ -0.6460 & 1.8246 & -0.1786 \\ -0.3624 & -0.1026 & 1.4650 \end{bmatrix}$$

respectively. The ultimate values and Ziegler-Nichols tuning parameters of the diagonal elements of this process transfer function matrix are shown in Table 7.4.3

Table 7.4.3 The ultimate values and ZN tuning parameters

Parameters	Loop 1	Loop 2	Loop 3
K_u	7.1317	-1.3935	12.4487
ω_u	0.6865	0.6266	1.7014
K_{ZN}	3.2417	-0.6334	5.6585
τ_{ZN}	7.6272	8.3564	3.0774

We assume that F and F_d are equal to 2.2 and 1 respectively and after executing the while loop in Appendix E the values of F and F_d become 2.19 and 2.18 respectively. At the same time, controller parameters can be calculated by using tuning factor F and F_d. See Table 7.4.4 for controller values. Table 7.4.4 shows the assumption and final values for F and F_d. In this case, we also find τ_D using F_d derivative factor.

Table 7.4.4 Tuning parameters

Parameter	Assumption	Final value
F	2.2	2.19
F_d	1	2.18

ETF based on DRGA: The critical frequencies of each loop are $\tilde{\omega}_{cr1} = 0.2564$ rad/s, $\tilde{\omega}_{cr2} = 0.2222$ rad/s and $\tilde{\omega}_{cr3} = 0.6667$ rad/s, respectively.

and

$$\rho_{11,2}(j0.2564) = -9.9431 - j13.7285$$

$$\rho_{22,2}(j0.2222) = 0.2948 + j3.4206$$

$$\rho_{33,2}(j0.6667) = -0.0729 - j0.0639$$

respectively. Subsequently MMF can be calculated as

$$\rho_{11,2} = 16.3844e^{-8.3779s}$$

$$\rho_{22,2} = 3.6575e^{-(-5.4402)s}$$

$$\rho_{33,2} = 0.9293e^{-0.1032s}$$

are used to fine-tune the PI/PID controller setting for all control loops. Then the equivalent transfer functions of all control loops are constructed as

$$\hat{g}_{11} = \frac{10.81e^{-11s}}{6.7s+1}$$
$$\hat{g}_{22} = \frac{-8.632e^{-3s}}{5s+1}$$
$$\hat{g}_{33} = \frac{0.87e^{-1.1s}}{10s+1}$$

Consequently, the decentralized PI controller parameters are determined by SIMC and shown in to Figure show the responses for each control loop.

RNGA: The gain and phase margin for all loops are specified to be 7 and $3\pi/7$ respectively. The DC gain, Critical Frequency Array, RGA, ERGA and RFA are

$$k = \begin{bmatrix} 0.6600 & -0.6100 & -0.0049 \\ 1.1100 & -2.3600 & -0.0100 \\ -34.6800 & 46.2000 & 0.8700 \end{bmatrix}, \quad \Omega = \begin{bmatrix} 0.6865 & 0.5123 & 1.6380 \\ 0.3521 & 0.6266 & 1.3927 \\ 0.2250 & 0.2108 & 1.6319 \end{bmatrix}$$

$$\Lambda = \begin{bmatrix} 2.0084 & -0.7220 & -0.2864 \\ -0.6460 & 1.8246 & -0.1786 \\ -0.3624 & -0.1026 & 1.4650 \end{bmatrix}, \quad \Phi = \begin{bmatrix} 1.2928 & -0.2026 & -0.0902 \\ -0.2076 & 1.2475 & -0.0399 \\ -0.0852 & -0.0449 & 1.1301 \end{bmatrix}$$

and

$$\Gamma = \begin{bmatrix} 0.6437 & 0.2806 & 0.3149 \\ 0.3213 & 0.6837 & 0.2237 \\ 0.2352 & 0.4377 & 0.7714 \end{bmatrix}$$

respectively.

Both RGA and ERGA pairing rules indicate diagonal pairing (NI =0.3859>0). Since $\lambda_{ii} > 1$ and $\gamma_{ii} < 1$ for $i = 1,2,3$, we do not need to detune and ETFs for two loops are

$$\hat{g}_{11}(s) = \frac{0.66e^{-2.6s}}{6.7s+1}, \quad \hat{g}_{22}(s) = \frac{-2.36e^{-3s}}{5s+1} \quad \text{and} \quad \hat{g}_{33}(s) = \frac{0.87e^{-s}}{10s+1}$$

respectively. The controller parameters for all methods are shown in 7.4.5. The closed-loop responses are shown in Figure 7.4.3, where the unit set-points change in r_1 at t=0, r_2 at t=400 and r_3 at t=800.

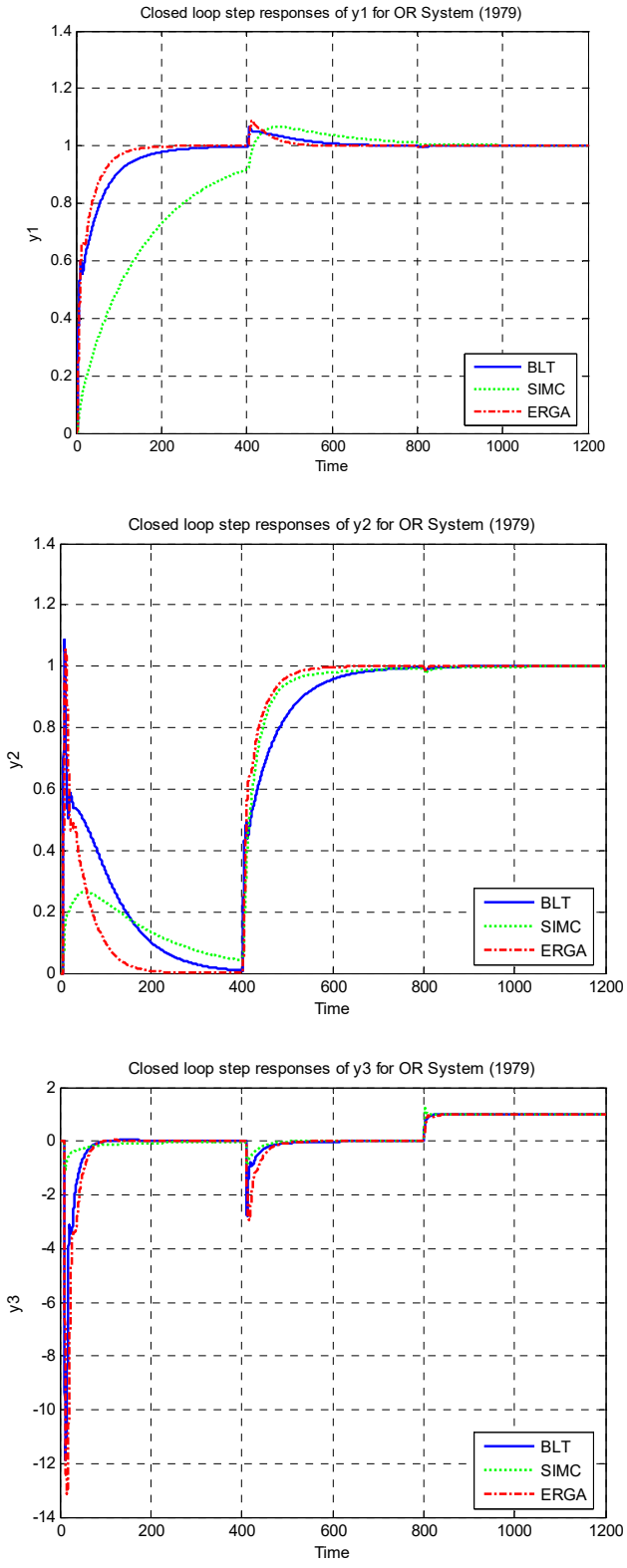

Figure 7.4.3 Closed loop step responses of OR system (1979)

Table 7.4.5 Decentralized Controllers for OR System

Method	Loop	K_P	τ_I	τ_D
BLT	1	1.4802	16.7038	1.1441
	2	-0.2892	18.3007	1.2535
	3	2.5838	6.7397	0.4616
SIMC	1	0.1334	6.7000	0
	2	-0.0938	5.0000	0
	3	6.9234	6.0000	0
REGA	1	0.8762	6.7000	0
	2	-0.1585	5.0000	0
	3	2.5793	10.0000	0

7.4.3 **Distillation Column 4×4 Model (**Alatiqi case 1) System

$$\mathbf{G}(s)=\begin{bmatrix} \dfrac{2.22e^{-2.5s}}{(36s+1)(25s+1)} & \dfrac{-2.94(7.9s+1)e^{-0.05s}}{(23.7s+1)^2} & \dfrac{0.017e^{-0.2s}}{(31.6s+1)(7s+1)} & \dfrac{-0.64e^{-20s}}{(29s+1)^2} \\ \dfrac{-2.33e^{-5s}}{(35s+1)^2} & \dfrac{3.46e^{-1.01s}}{32s+1} & \dfrac{-0.51e^{-7.5s}}{(32s+1)^2} & \dfrac{1.68e^{-2s}}{(28s+1)^2} \\ \dfrac{-1.06e^{-22s}}{(17s+1)^2} & \dfrac{3.511e^{-13s}}{(12s+1)^2} & \dfrac{4.41e^{-1.01s}}{16.2s+1} & \dfrac{-5.38e^{-0.5s}}{17s+1} \\ \dfrac{-5.73e^{-2.5s}}{(8s+1)(50s+1)} & \dfrac{4.32(25s+1)e^{-0.01s}}{(50s+1)(5s+1)} & \dfrac{-1.25e^{-2.8s}}{(43.6s+1)(9s+1)} & \dfrac{4.78e^{-1.15s}}{(48s+1)(5s+1)} \end{bmatrix}$$

The elements $g_{12}(s)$ and $g_{42}(s)$ in this process are not standard models. They have zeros at $s=-0.1266$ and $s=-0.0400$ respectively.

$$\Lambda=\begin{bmatrix} 3.5280 & -1.0766 & 0.0502 & -1.5016 \\ -3.3628 & 2.7685 & -0.7028 & 2.2971 \\ -0.1203 & 0.1305 & 2.2635 & -1.2736 \\ 0.9552 & -0.8224 & -0.6109 & 1.4781 \end{bmatrix}$$

respectively.

BLT: The ultimate values and Ziegler-Nichols tuning parameters of the diagonal elements of this process transfer function matrix are shown in Table 7.4.6

Table 7.4.6 The ultimate values and ZN tuning parameters

Parameters	Loop 1	Loop 2	Loop 3	Loop 4
K_u	11.3027	14.5683	5.8583	10.0365
ω_u	0.1634	1.5749	1.5936	0.4250
K_{ZN}	5.1376	6.6219	2.6629	4.5620
τ_{ZN}	32.0454	3.3247	3.2857	12.3190

We assume that F and F_d are equal to 2.5 and 1 respectively, and after executing the while loop in Appendix F the values of F and F_d become 2.49 and 1 respectively. At the same time, controller parameters can be calculated by using tuning factors F and F_d. See Table 7.4.7 for controller values. The following table shows the assumption and final values for F and F_d.

Table 7.4.7 Tuning parameters

Parameter	Assumption	Final value
F	2.5	1
F_d	2.49	1

In this case, we also find τ_D using F_d derivative factor.

ETF based on DRGA: The critical frequencies for all control loops as

$$\tilde{\omega}_{cr1} = 0.1333 \text{ rad/s},$$

$$\tilde{\omega}_{cr2} = 0.3300 \text{ rad/s},$$

$$\tilde{\omega}_{cr3} = 0.3300 \text{ rad/s}$$

and

$$\tilde{\omega}_{cr4} = 0.2899 \text{ rad/s}$$

respectively. and

$$\delta_{11}(j0.1333) = 0.2244 + j0.5093$$

$$\delta_{22}(j0.3300) = -0.0084 + j0.0083$$

$$\delta_{33}(j0.3300) = 0.0023 - j0.0022$$

$$\delta_{44}(j0.2899) = -0.0256 + j0.2630$$

respectively. Subsequently MMF can be calculated as

$$\rho_{11} = 1.3261e^{-(-2.9566)s}; \qquad \rho_{22} = 0.9916e^{-(-0.0255)s}$$
$$\rho_{33} = 1.0023e^{-0.0066s}; \qquad \rho_{44} = 1.0093e^{-(-0.9094)s}$$

Then the equivalent transfer functions of all control loops are constructed as

$$\hat{g}_{11} = \frac{2.944e^{-2.5s}}{900s^2 + 61s + 1}; \qquad \hat{g}_{22} = \frac{-3.46e^{-1.01s}}{32\ \mathrm{s} + 1}$$
$$\hat{g}_{33} = \frac{4.42e^{-1.02s}}{16.2\ \mathrm{s} + 1}; \qquad \hat{g}_{44} = \frac{4.824e^{-1.15s}}{240s^2 + 53s + 1}$$

Consequently, the decentralized PI controller parameters are determined by SIMC and shown in Table 7.4.8 and Figure 7.4.4 show the responses for each control loop.

RNGA: The gain and phase margin for all loops are specified to be 5 and $2\pi/5$ respectively. The DC gain, Critical Frequency Array, RGA, ERGA and RFA are

$$k = \begin{bmatrix} 2.2200 & -2.9400 & 0.0170 & -0.6400 \\ -2.3300 & 3.4600 & -0.5100 & 1.6800 \\ -1.0600 & 3.5110 & 4.4100 & -5.3800 \\ -5.7300 & 4.3200 & -1.2500 & 4.7800 \end{bmatrix}, \quad \Omega = \begin{bmatrix} 0.0209 & 0.0249 & 0.0302 & 0.0221 \\ 0.0183 & 0.0312 & 0.0200 & 0.0229 \\ 0.0377 & 0.0534 & 0.0616 & 0.0587 \\ 0.0195 & 0.0356 & 0.0219 & 0.0206 \end{bmatrix},$$

$$\Lambda = \begin{bmatrix} 3.5280 & -1.0766 & 0.0502 & -1.5016 \\ -3.3628 & 2.7685 & -0.7028 & 2.2971 \\ -0.1203 & 0.1305 & 2.2635 & -1.2736 \\ 0.9552 & -0.8224 & -0.6109 & 1.4781 \end{bmatrix}, \quad \Phi = \begin{bmatrix} 1.8820 & 0.1371 & 0.0487 & -1.0678 \\ -1.4541 & 2.1913 & 0.0159 & 0.2469 \\ -0.0265 & -0.0174 & 1.9648 & -0.9209 \\ 0.5987 & -1.3110 & -1.0294 & 2.7417 \end{bmatrix}$$

and

$$\Gamma = \begin{bmatrix} 0.5334 & -0.1273 & 0.9710 & 0.7111 \\ 0.4324 & 0.7915 & -0.0226 & 0.1075 \\ 0.2203 & -0.1330 & 0.8680 & 0.7231 \\ 0.6267 & 1.5942 & 1.6850 & 1.8549 \end{bmatrix}$$

respectively.

Both RGA and ERGA pairing rules indicate diagonal pairing (NI =0.1193>0). Since $\lambda_{ii} > 1$ and $\gamma_{ii} < 1$ for $i = 1,2,3$, we do not need to detune for those loops but for $\lambda_{ii} > 1$ and $\gamma_{ii} > 1$ for $i = 4$ we need to detune and, ETFs are

$$\hat{g}_{11}(s) = \frac{2.22e^{-2.5s}}{900s^2 + 61s + 1}, \qquad \hat{g}_{22}(s) = \frac{3.46e^{-1.01s}}{32\ \mathrm{s} + 1}, \qquad \hat{g}_{33}(s) = \frac{4.41e^{-1.01s}}{16.2\ \mathrm{s} + 1}$$

and

$$\hat{g}_{44}(s) = \frac{4.78e^{-2.13s}}{240s^2 + 53s + 1}$$

respectively. The controller parameters for all methods are shown in Table 7.4.8.

Table 7.4.8 Decentralized Controllers for A1 System

Method	Loop	K_C	τ_I	τ_D
BLT	1	2.0632	79.7944	4.8068
	2	2.6594	8.2786	0.4987
	3	1.0694	8.1816	0.4929
	4	1.8321	30.6749	1.8479
SIMC	1	1.6305	30.0000	25.0000
	2	3.0523	12.1200	0
	3	1.2070	12.1462	0
	4	2.8838	13.8000	5.0000
ERGA	1	3.4529	61.0000	14.7541
	2	2.8768	32.0000	0
	3	1.1426	16.2000	0
	4	1.6330	53.0000	4.5283

Figure 7.4.7 shows the responses for all control methods with unit set points change in r_1 at t=0, r_2 at t=400, r_3 at t=800 and r_4 at t=1200.

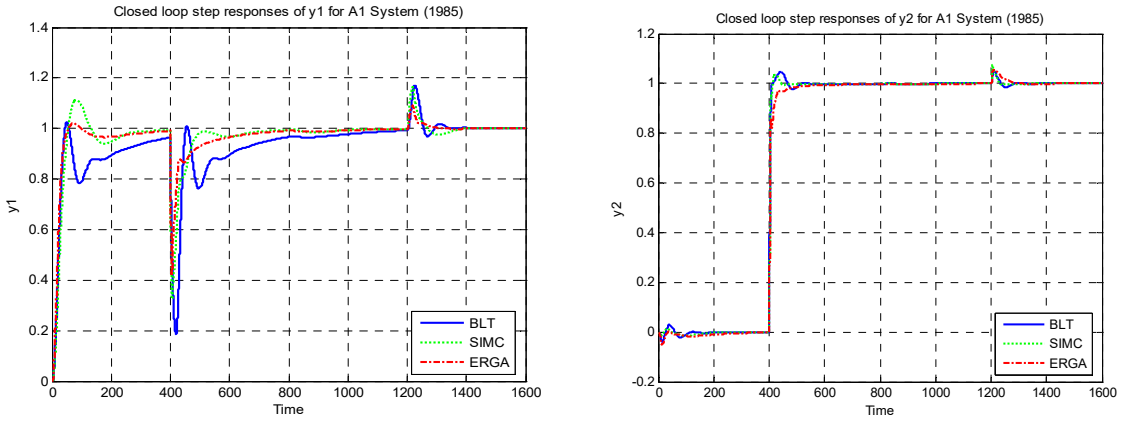

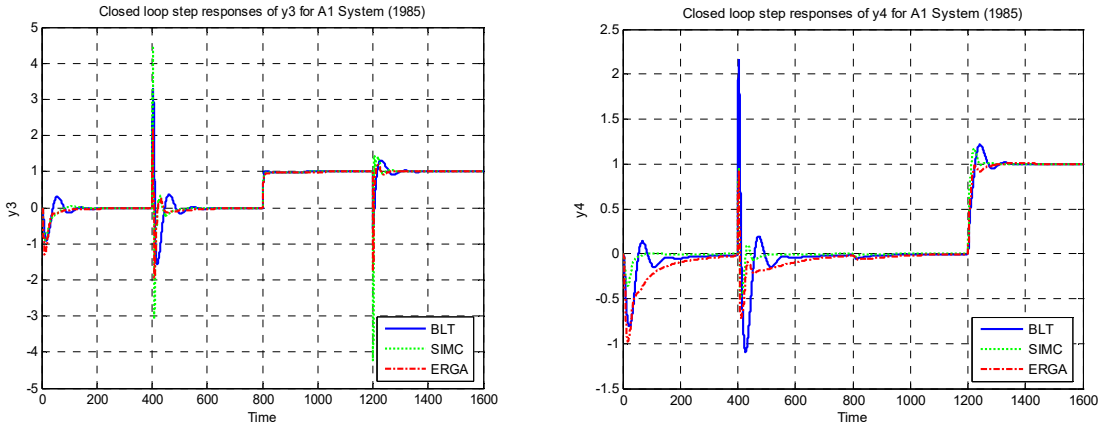

Figure 7.4.4 Step responses of A1 System (1985)

7.4.4 Performance Analysis

To evaluate the output control performance, we consider a unit step set point change for each loop, and the integrated absolute error (IAE), the integrated square error (ISE) and the integrated time absolute error (ITAE) of $e_i = y_i - r_i$ are used to evaluate the control performance such that

$$IAE = \int_0^\infty |e_i| \, dt \tag{7.4.1}$$

$$ISE = \int_0^\infty e_i^2 dt \tag{7.4.2}$$

and

$$ITAE = \int_0^\infty |e_i| \times t_i \, dt \tag{7.4.3}$$

respectively. These codes will generate the contents of Table 7.4.9 to 7.4.11.

Table 7.4.9 Performance Analysis for VL System

Methods	Controller	IAE	ISE	ITAE
BLT	Loop 1	6.700269	3.041136	113.736678
	Loop 2	2.142164	0.890127	73.807713
DRGA	Loop 1	11.055941	4.879077	215.310918
	Loop 2	2.104946	0.810928	64.872263
RNGA	Loop 1	4.141611	2.054463	65.335278
	Loop 2	2.541929	0.827885	71.617611

Table 7.4.10 Performance Analysis for OR System

Methods	Controller	IAE	ISE	ITAE
BLT	Loop 1	40.669637	11.913219	5207.841148
	Loop 2	122.673663	47.662144	29961.832043
	Loop 3	213.878712	1092.095839	29028.759469
SIMC	Loop 1	154.647127	71.142149	26730.952140
	Loop 2	90.409888	24.020309	24398.624396
	Loop 3	65.994708	19.914998	16407.995639
ERGA	Loop 1	31.766417	11.258064	3374.608357
	Loop 2	70.727090	31.085399	14662.244667
	Loop 3	350.391320	2003.041302	48476.558050

Table 7.4.11 Performance Analysis for A1 System (1985)

Methods	Controller	IAE	ISE	ITAE
BLT	Loop 1	127.399980	40.959631	52132.564747
	Loop 2	9.684995	2.088477	4766.423058
	Loop 3	135.942491	131.136045	65605.190341
	Loop 4	130.146470	78.475350	61284.463291
SIMC	Loop 1	91.620452	36.804210	33937.547835
	Loop 2	7.910612	2.182851	4095.297639
	Loop 3	90.242356	95.401712	43643.197559
	Loop 4	41.880308	12.395012	21448.368157
ERGA	Loop 1	59.343257	19.869040	20765.241418
	Loop 2	15.798839	2.746638	8191.105350
	Loop 3	102.073710	77.894160	44768.557853
	Loop 4	146.755354	50.885016	57869.975745